

## Electronic structure of quasicrystals deduced from Auger and x-ray photoelectron spectroscopies

This article has been downloaded from IOPscience. Please scroll down to see the full text article.

2002 J. Phys.: Condens. Matter 14 2691

(<http://iopscience.iop.org/0953-8984/14/10/318>)

View [the table of contents for this issue](#), or go to the [journal homepage](#) for more

Download details:

IP Address: 171.66.16.27

The article was downloaded on 17/05/2010 at 06:18

Please note that [terms and conditions apply](#).

# Electronic structure of quasicrystals deduced from Auger and x-ray photoelectron spectroscopies

V Fourn e<sup>1,3</sup>, J W Andereg g<sup>1</sup>, A R Ross<sup>1,2</sup>, T A Lograsso<sup>1,2</sup> and P A Thiel<sup>1,3</sup>

<sup>1</sup> Ames Laboratory, Iowa State University, Ames, IA 50011, USA

<sup>2</sup> Department of Materials Science and Engineering, Iowa State University, Ames, IA 50011, USA

<sup>3</sup> Department of Chemistry, Iowa State University, Ames, IA 50011, USA

E-mail: thiel@ameslab.gov

Received 13 December 2001

Published 18 March 2002

Online at [stacks.iop.org/JPhysCM/14/2691](http://stacks.iop.org/JPhysCM/14/2691)

## Abstract

Specific features in the electronic structure of Al–transition metal quasicrystals are analysed by a combination of Auger and x-ray photoelectron spectroscopies. We first demonstrate that different degrees of asymmetry in the transition metals' 2p core-level lineshape observed across different types of surface structure correspond to variations in the density of states at the Fermi level,  $\text{DOS}(E_F)$ . Using this effect, we explore the controversial issue of whether the quasicrystalline, decagonal AlNiCo system is electronically stabilized. We find strong evidence for the presence of a reduced  $\text{DOS}(E_F)$  in this system, as expected for electronically stabilized compounds, and as observed in the quasicrystalline, icosahedral AlPdMn and AlCuFe alloys. Finally, qualitative information on the nature of the electronic states in quasiperiodic structures extracted from the core–valence–valence Auger lines are presented and discussed.

## 1. Introduction

Quasicrystals (QCs) are long-range-ordered, aperiodic solids, usually with fivefold or tenfold rotational symmetry [1]. Their unique atomic structure is associated with an unusual combination of physical properties that makes them useful in a number of technological applications [2]. It also correlates with interesting aspects of their electronic structure. In this paper, we focus on that electronic structure.

The Al-rich quasicrystalline alloys that are the subject of this article are stable icosahedral and decagonal phases. They exhibit quasicrystallinity in three and two dimensions, respectively. Their stability is usually assumed to arise from a Hume-Rothery type of mechanism, where the total energy of the system is lowered by a structure-induced minimum in the density of states (DOS) at the Fermi level ( $E_F$ ), termed a pseudogap [3]. The pseudogap

arises from the matching between the Fermi sphere and strongly scattering Bragg planes that define the equivalent of a Brillouin zone for a QC. The scattering by the Bragg planes is enhanced by *sp*-*d* hybridization effects, resulting in a larger Fermi surface–Brillouin zone interaction [4, 5]. These materials also present some unexpected electron transport properties, different from those of both amorphous and crystalline alloys. Low values of conductivity are typical, and the values decrease when temperature decreases, contrary to usual metallic behaviour [6]. This suggests a certain degree of localization of the electronic states responsible for the conduction, i.e. of states having an energy close to  $E_F$ . Also, the existence of critical states decaying as a power-law function has been predicted for a quasiperiodic potential [7]. Such electrons would be neither truly localized nor extended. They could tunnel from one region of diameter  $d$  to another region having the same local environment, as these two regions should always be no further apart than  $2d$  according to the Conway theorem for quasiperiodic structures [8].

These general properties of QCs have generated strong interest in their electronic structure. This structure is usually probed by photoemission spectroscopy (PES) of the valence band or by soft x-ray emission spectroscopy (SXES). The ultimate goal here is to check for the existence of the reduced DOS( $E_F$ ) expected for electronic compounds. In photoemission studies of the valence band, the energy distribution of the photoelectrons reflects the sum of the partial DOS of each elemental species weighted by the corresponding photoionization cross-sections. High energy resolution in the vicinity of the Fermi edge is necessary to assess the presence or absence of the pseudogap. Even when the experimental requirements for high resolution are fulfilled, the situation is not always unambiguous. On the other hand, SXES is a momentum- and site-selective technique which therefore has the advantage that it can resolve each partial DOS separately and for each element in the compound. But the energy resolution achievable in SXES is intrinsically limited by the width of the core level involved in the x-ray transition process. Nonetheless, strong support for the presence of a pseudogap in several Al-based quasicrystalline phases has been derived from SXES based on the observation of a shift of the Al partial electronic distributions below the Fermi level, with a consequent reduction of the spectral intensity at  $E_F$  [9].

Although less direct, useful information on the electronic structure of QCs can also be gained from PES of the core levels and from Auger electron spectroscopy (AES) measurements. Indeed, deep core levels are less sensitive to their chemical environment than the valence levels, but signatures of the external medium in which the atoms are embedded can be found in the spectral features through their positions (binding energies, BE), their shape, or their satellite structure [10]. In that respect, the asymmetric shape of the core-level lines in metallic systems is of particular interest as it is directly correlated with the local DOS( $E_F$ ) around the atoms where the photoelectrons are produced [11]. The Auger transitions involving the valence levels, especially the core–valence–valence (CVV) lines, are also of interest as their shape normally reflects the self-convolution of the valence band, and departure from this band-like behaviour might contain information on the degree of correlation between the valence electrons [12].

In a previous paper, we presented an analysis of the Mn and Fe 2p core-level lines in several crystalline and quasicrystalline structures of the Al–Pd–Mn and Al–Cu–Fe ternary systems [13]. In the present paper, we elaborate upon the analysis of the data for these systems, presenting a more complete comparison than given previously. Further, we use this as a background for extending the lineshape analysis to the Al–Ni–Co decagonal phase. We also include a description of the satellite structure in the Ni spectra. This more exhaustive approach leads us to the conclusion that the 2p core levels of transition metals (TMs) consistently lose their asymmetric tail, providing indirect—but reliable—evidence that a pseudogap exists at the Fermi energy, both in icosahedral and decagonal QCs. We will further present some results

concerning the CVV Auger lines of TMs in the Al–Pd–Mn and Al–Cu–Fe icosahedral phases as well as in the Al–Ni–Co decagonal QC.

## 2. Experimental description

Two single-grain icosahedral samples with the chemical compositions  $\text{Al}_{72}\text{Pd}_{19.5}\text{Mn}_{8.5}$  and  $\text{Al}_{63.4}\text{Cu}_{24}\text{Fe}_{12.6}$  were prepared by the Bridgman method and by liquid-assisted growth, respectively [14, 15]. Then a surface oriented perpendicularly to a fivefold symmetry axis was selected and mechanically polished using diamond paste and Mastertex<sup>®</sup> cloth down to a final roughness of  $0.25\ \mu\text{m}$ . We also used an  $\text{Al}_{72}\text{Ni}_{11}\text{Co}_{17}$  decagonal quasicrystalline sample grown by a flux method (slow cooling) from which a tenfold surface was prepared in a similar way [16]. The chemical compositions were verified by energy-dispersive x-ray spectroscopy (EDX) and agree well with the results of a quantitative analysis by XPS using uncalibrated sensitivity factors, at least within the experimental accuracies (about  $\pm 2\%$ ) of these two techniques and except for AlNiCo, where the overlap between core and Auger lines makes the analysis impossible. A clean surface was prepared in UHV by cycles of  $\text{Ar}^+$  sputtering and annealing ( $500\ ^\circ\text{C}$  for AlCuFe,  $600\ ^\circ\text{C}$  for AlPdMn,  $700\ ^\circ\text{C}$  for AlNiCo). These preparation conditions are known to yield a terrace and step surface morphology that corresponds to a 2D cross-section of the bulk structure with no reconstruction and no faceting (i.e. bulk-terminated surface), as demonstrated by recent atomically resolved scanning tunnelling microscopy images [17–19].

For the sake of comparison across different types of structure, we used several Al–Pd–Mn ternary alloys, including the  $\xi'$ -approximant and two other crystals,  $\text{Al}_{60}\text{Pd}_{25}\text{Mn}_{15}$  and  $\text{Al}_6\text{Mn}$ . Details of these samples have already been given in [13].

The photoelectron spectra were acquired using a Perkin–Elmer Multitechnique Chamber, Model 5500, fitted with an Omni Focus III lens system, and monitored with PHI-ACCESS software. The x-ray source was either a monochromatized Al  $K\alpha$  radiation or a standard Mg  $K\alpha$  radiation if required by the overlapping between Auger and core-level lines. The take-off angle was set to  $45^\circ$ . Under these conditions, XPS and x-ray-induced Auger electron spectroscopy (XAES) measurements provide a depth-weighted average over the top 20–25 Å of material, which is the surface/near-surface region. Energy calibration of the spectrometer was achieved using the Au  $4f_{7/2}$  (84.0 eV) and Cu  $2p_{3/2}$  (932.7 eV) lines. The resolution was 0.65 eV for the Al  $K\alpha$  source and 1.1 eV for the Mg  $K\alpha$  source, using in both cases a pass energy of 29.5 eV. The XPS valence bands presented here were corrected for secondary-electron background.

## 3. Results

### 3.1. AlPdMn and AlCuFe icosahedral phases

The XPS VB spectra of the AlPdMn and AlCuFe icosahedral phases, measured at liquid nitrogen temperature, are shown in figures 1(a) and (b). These alloys have similar atomic and electronic structures. The main peak, 4 eV below  $E_F$ , is due to Pd 4d (figure 1(a)) and Cu 3d (figure 1(b)) states, respectively. The Mn 3d and Fe 3d states contribute to the spectral intensity closer to  $E_F$  [9, 20]. The broader contribution from Al sp states is not visible in these spectra due to photoionization cross-sections being much smaller for sp states than for d states. The pseudogap at  $E_F$ , observed as a dip in several ultrahigh-energy-resolution photoemission spectra of the VBs of these compounds, is therefore essentially due to a reduced local DOS at  $E_F$  ( $\text{LDOS}(E_F)$ ) around Mn or Fe atoms [21, 22]. (The energy resolution in the experiments of figure 1 is too low to allow such an analysis from the present data.) We show below that

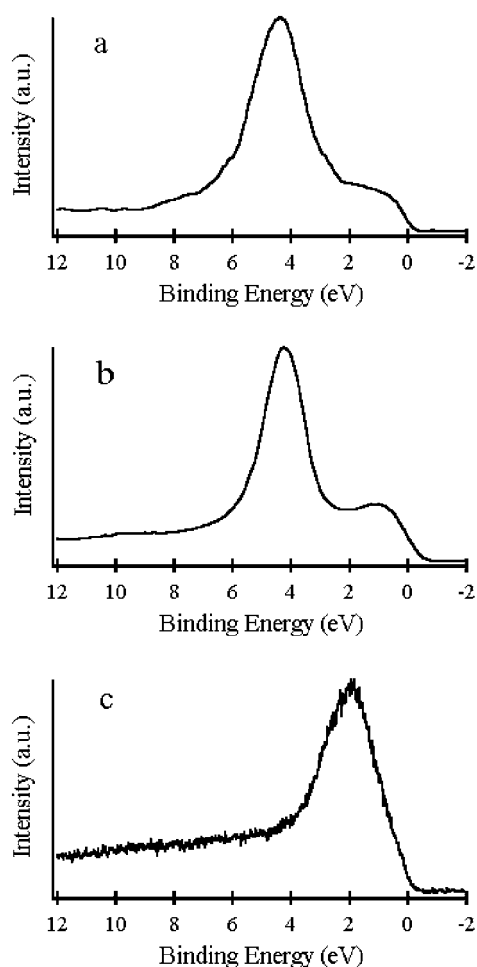


**Figure 1.** XPS VB spectra measured at liquid nitrogen temperature for *i*-Al<sub>72</sub>Pd<sub>19.5</sub>Mn<sub>8.5</sub> (*a*), for *i*-Al<sub>63.4</sub>Cu<sub>24</sub>Fe<sub>12.6</sub> (*b*), and for *d*-Al<sub>72</sub>Ni<sub>11</sub>Co<sub>17</sub> (*c*) quasicrystalline phases.

this pseudogap is correlated with a reduced asymmetry of the Mn 2p and Fe 2p core-level lines measured by XPS.

We recall first that the asymmetric shape of core-level spectra in metallic systems arises from electron–hole (e/h) excitation across the Fermi edge [23]. The photoelectron emitted from a deep core level can lose a bit of its kinetic energy to excite electrons from levels just below  $E_F$  into the first unoccupied states above  $E_F$ . The probability of these excitations decreases rapidly with the e/h pair energy, so it is essentially a Fermi surface excitation process. Different degrees of asymmetry can then be understood because the probability of an e/h pair excitation will depend on the number of electronic states available in the vicinity of  $E_F$ . This implies that the asymmetry of the XPS core-level lines depends on the LDOS( $E_F$ ). This effect can be used as a tool to probe the valence electrons in metallic compounds.

Experimentally, the asymmetry parameter  $\alpha$  is derived by fitting the experimental function with a Gaussian experimental function convoluted with a Doniach–Sunjic lineshape, and a Shirley background is used to account for the emission of secondary electrons [24]. We find

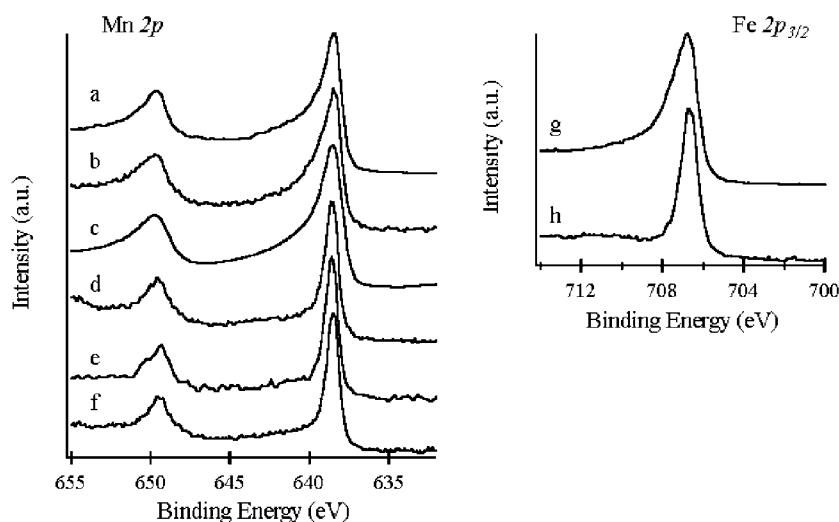


**Figure 2.** Left: Mn 2p core levels of (a) the pure Mn surface, (b) the cubic  $\text{Al}_{57}\text{Pd}_{36}\text{Mn}_7$  surface, (c) the  $i\text{-Al}_{72}\text{Pd}_{19.5}\text{Mn}_{8.5}$  surface prepared by sputtering and annealing at 540 K to yield a cubic overlayer with composition  $\text{Al}_{59}\text{Pd}_{35}\text{Mn}_6$ , (d) the orthorhombic  $\text{Al}_6\text{Mn}$  crystal, (e) the  $\xi'\text{-Al}_{73}\text{Pd}_{22.5}\text{Mn}_{4.5}$  approximant phase, and (f) the  $i\text{-Al}_{72}\text{Pd}_{19.5}\text{Mn}_{8.5}$  surface prepared by fracture in UHV. Right: Fe  $2p_{3/2}$  core levels of (g) the pure Fe(110) and (h) the  $i\text{-Al}_{63.4}\text{Cu}_{24}\text{Fe}_{12.6}$  surface prepared by sputtering and annealing at 770 K.

that using an integrated background or a polynomial background gives some small variations in the values of  $\alpha$  but does not modify the robust trends that we will describe in the following. More details about the fitting procedure are given elsewhere [13].

We summarize the results of [13] for the AlPdMn and AlCuFe systems in figure 2. The Mn 2p core-level lines in for pure Mn metal and for the several AlPdMn crystalline, approximant, or icosahedral phases are shown in figure 2 (left). The Fe 2p core-level lines for the pure Fe metal and for the icosahedral AlCuFe are shown in figure 2 (right). Residuals show that the quality of the fit using the Doniach–Sunjic lineshape is good [13].

The lines have a pronounced asymmetry for the pure Mn and Fe metals, which is quantified by the parameter  $\alpha$  derived from the fit. The numerical values of  $\alpha$ , the intrinsic linewidth  $2\gamma$ , and the BE are listed in table 1. Both Mn and Fe TMs are characterized by an unfilled d band dominating their electronic structure implying a high  $\text{DOS}(E_F)$ . The asymmetric tail of the core line could therefore reasonably be ascribed to the effect of  $e/h$  excitations across  $E_F$ . One could also argue that the tail arises from a multiplet structure because of the presence of unpaired electrons in the  $3d^5$  or  $3d^6$  open-valence-shell configuration of Mn and Fe. Although this is true in principle, only in TM oxides or dihalides have multiplet structures been observed experimentally or predicted theoretically in 2p, 3s and 3p levels, with satellite peaks clearly separated from the main line by several eV [25, 26]. To our knowledge, there are no reports of high-energy-resolution spectra of the Mn, Fe, or Co 2p core levels showing any multiplet splitting in a metallic system. Hence, we regard it as improbable (although not impossible) that the asymmetry of the line could be due to a series of electronic levels with small energy separation that could not be resolved experimentally.

A high degree of asymmetry is also observed in the spectra for the cubic AlPdMn crystal, for the disordered surface prepared by sputtering only, and for the sputtered surface annealed at a temperature below 700 K and whose LEED pattern exhibits a cubic symmetry [27]. In these

**Table 1.** Fitting parameters corresponding to the data of figures 2–4.  $E_B$  is the BE of the core level,  $\alpha$  is the asymmetry parameter,  $2\gamma$  is the intrinsic width.

Sample	$E_B$ (eV)	$\alpha$	$2\gamma$ (eV)
Mn 2p <sub>3/2</sub> in pure Mn	638.3	0.46	0.38
Mn 2p <sub>3/2</sub> in cubic Al <sub>57</sub> Pd <sub>36</sub> Mn <sub>7</sub>	638.2	0.43	0.53
Mn 2p <sub>3/2</sub> in i-Al <sub>72</sub> Pd <sub>19.5</sub> Mn <sub>8.5</sub> sputter-annealed at 540 K (cubic surface)	638.2	0.43	0.51
Mn 2p <sub>3/2</sub> in o-Al <sub>6</sub> Mn	638.5	0.23	0.27
Mn 2p <sub>3/2</sub> in $\xi'$ -Al <sub>73</sub> Pd <sub>22.5</sub> Mn <sub>4.5</sub>	638.5	0.17	0.29
Mn 2p <sub>3/2</sub> in i-Al <sub>72</sub> Pd <sub>19.5</sub> Mn <sub>8.5</sub> prepared by fracture (pentagonal surface)	638.4	0.18	0.29
Fe 2p <sub>3/2</sub> in pure Fe(110)	706.6	0.38	0.50
Fe 2p <sub>3/2</sub> in i-Al <sub>63.4</sub> Cu <sub>24</sub> Fe <sub>12.6</sub>	706.6	0.10	0.40
Ni 2p <sub>3/2</sub> in pure Ni	852.65	0.20	0.68
Ni 2p <sub>3/2</sub> in d-Al <sub>72</sub> Ni <sub>11</sub> Co <sub>17</sub>	853.8	0.05	0.68
Co 2p <sub>3/2</sub> in pure Co	778.15	0.27	0.49
Co 2p <sub>3/2</sub> in d-Al <sub>72</sub> Ni <sub>11</sub> Co <sub>17</sub>	778.65	0.07	0.34

cases, as in the pure metals, the asymmetry of the core-level lines is correlated directly with a sharp metallic Fermi edge in the VB spectra [22].

A weaker asymmetry is clearly visible ‘by eye’ in the lineshape of the i-AlCuFe, the i-AlPdMn, and the approximant phases o-Al<sub>6</sub>Mn and  $\xi'$ -AlPdMn. This is further quantified by the values of  $\alpha$  returned by the fit (see table 1). Consistently, the reduced asymmetry can be correlated with direct observations of a pseudogap at the Fermi edge for both icosahedral phases [28] or with the calculated electronic structure for the o-Al<sub>6</sub>Mn crystal [29]. We also reported recently that the asymmetry of the Mn 2p lines increases with increasing surface sensitivity for an i-AlPdMn QC surface prepared by fracture in UHV [13]. The same effect was also observed by Neuhold *et al* [30] for the Al 2p line on the same sample, indicating an enhanced metallic character at the fractured surface. If the asymmetric tail of the TM 2p levels were due to an unresolved multiplet structure, it would be difficult to understand why this structure changes with the surface sensitivity. This further substantiates our interpretation that the physical mechanism responsible for the suppression of the asymmetric tail of the 2p core levels of TMs in these alloys is a reduced DOS( $E_F$ )—i.e. opening of the pseudogap—rather than multiplet splitting effects, in agreement with an electronic stabilization of QCs and approximants.

The core levels of Cu and Pd undergo a similar loss of the asymmetric tail in QC phases. This is expected from the positions of their d bands which lie about 4 eV below  $E_F$  (see figure 1), with therefore little DOS remaining at  $E_F$ . The filling of the Cu and Pd d bands, and their corresponding shift toward higher BE upon alloying with Al, is not specific to QCs and has been observed in many systems, such as crystalline Al–Cu and Al–Pd alloys [5, 31]. We do not discuss their case further, as they are of less interest.

### 3.2. AlNiCo decagonal phase

The XPS VB spectrum measured at liquid nitrogen temperature is shown figure 1(c). It is composed of a main peak corresponding to the overlapping Ni 3d-like and Co 3d-like

states whose centre is located about 2 eV below  $E_F$ . Again, due to large differences in the photoionization cross-sections, the contribution of s- and p-like states of Al, Ni, and Co atoms are largely obscured. The low-energy resolution of this experiment precludes an analysis of the presence or absence of the pseudogap feature. Previous measurements of the VB by means of photoemission led to contradictory results. With an energy resolution of 0.4 eV, it was first concluded that no pseudogap exists in the  $\text{Al}_{70}\text{Ni}_{15}\text{Co}_{15}$  decagonal phase [32], but a later ultrahigh-energy-resolution experiment on the same alloy suggested the opposite result [28]. This is based on a successful fitting of the Fermi edge with the pseudogap function:

$$I(E) = \int N(ax + b)(1 - C \exp(-x/2\sigma^2))f(x, T)G_{\text{exp}}(x, E) dx. \quad (1)$$

This procedure, however, assumes that the DOS in the vicinity of  $E_F$  can be approximated as a linear function, modulated by a Lorentzian dip to mimic the pseudogap at  $E_F$ . The Fermi–Dirac distribution at the temperature  $T$  of the measurement and a Gaussian experimental broadening are also taken into account in this procedure. In the case of the  $\text{AlNiCo}$  decagonal phase, it is difficult and ambiguous to assume a linear variation of the DOS in the vicinity of  $E_F$ , as the Co and Ni d states are located in this energy range.

We mention also that band-structure calculations have been performed by Krajci *et al* [33] on a periodic approximant  $\text{Al}_{70}\text{Ni}_{15}\text{Co}_{15}$  containing as many as 1276 atoms in an orthorhombic unit cell. Their results show that the details of the VB structure in the vicinity of  $E_F$  strongly depend on details of the short-range chemical order, and it is therefore difficult to assess the question of the pseudogap in the decagonal phase.

Considering this issue, we measured the Ni  $2p_{3/2}$  core-level spectra for pure Ni and for the decagonal phase. They are shown in figure 3. For the metal, the main line is accompanied by the so-called ‘6 eV satellite’ peak [10]. The origin of this satellite is as follows. In the initial state of the photoemission process, the Ni 3d band is not completely filled and therefore some Ni 3d character remains above  $E_F$ . The Ni 3d band also falls in the middle of the wide Ni 4s band. In the final state, the hole in the  $2p_{3/2}$  level produces an additional Coulomb attraction that pulls the electronic levels below  $E_F$ . An additional screening electron can occupy a d orbital, thus leading to a final-state  $3d^{10}$  configuration. This state, where the Ni d band is fully occupied, corresponds to the main line. The satellite peak corresponds to a  $3d^9$  final-state configuration where, although the Ni d band is now fully below  $E_F$ , it is not filled by an additional screening electron. The wide Ni 4s band instead produces the screening. In this situation, there are still some unoccupied states with Ni d character above  $E_F$ , and their weight and position are known to determine the intensity of the satellite [31]. Figure 3 clearly shows that the satellite has completely vanished in the decagonal phase, suggesting that the Ni d band is filled in the QC. The  $\text{LDOS}(E_F)$  around Ni atoms should then be reduced as a result of the band filling, and the asymmetric tail of the Ni  $2p_{3/2}$  core-level line produced by e/h pair excitations should be less pronounced. This is indeed observed in figure 3 and further quantified by the values of the index  $\alpha$  deduced from the fit. We only can use these values of  $\alpha$  for qualitative comparison, as the presence of the satellite in pure Ni may contribute to a slight increase in the asymmetry of the main Ni line.

The filling of the Ni d band also correlates with a chemical shift of 1.1 eV of the Ni  $2p_{3/2}$  line in the QC. This is not specific to this quasicrystalline phase, as it is also observed for the  $\text{Al}_3\text{Ni}_2$  and  $\text{Al}_3\text{Ni}$  crystalline phases [31]. In reference [31], it could also be directly observed as a shift of the Ni d band in the VB spectra. Such an observation is not possible in our case because of the overlap between Co and Ni d states in the VB spectra. A smaller asymmetry parameter for the Co  $2p_{3/2}$  core-level spectrum for the decagonal phase as compared to the



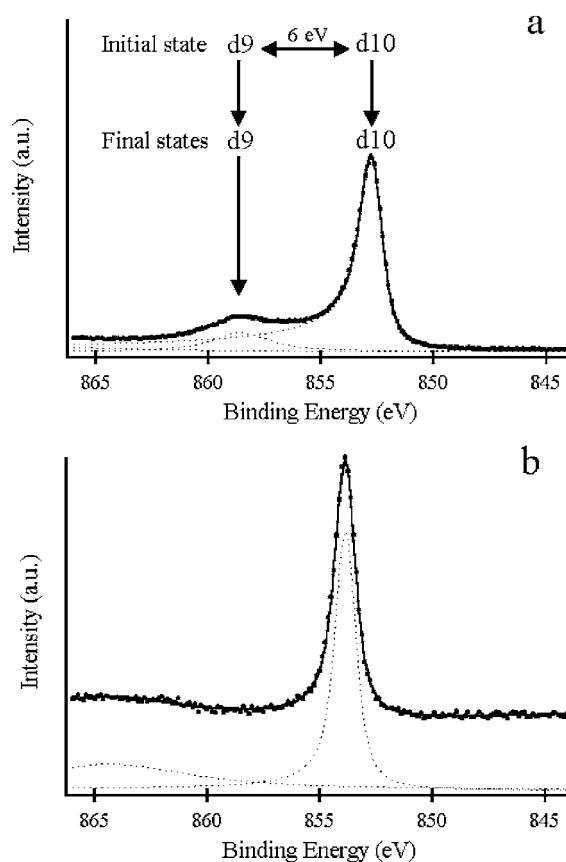


**Figure 3.** Ni  $2p_{3/2}$  core levels (a) in pure Ni and (b) in d-Al<sub>72</sub>Ni<sub>11</sub>Co<sub>17</sub>.

pure Co is also observed in figure 4. The intrinsic width of the line is also smaller for the QC and a chemical shift of 0.5 eV is measured.

The observation of a reduced LDOS( $E_F$ ) around the Ni and Co atoms is very much consistent with the existence of a pseudogap at  $E_F$ , as the Ni and Co d-like states should represent the main contribution to the DOS. Additional support for the existence of a pseudogap in the decagonal AlNiCo phase is given by SXES experiments on the same class of alloys, which show that the spectral distributions of Al sp states are shifted from  $E_F$ . This provides evidence of a reduced LDOS( $E_F$ ) also around Al atoms [34]. A smaller asymmetry parameter  $\alpha$  of the Al 2p core levels should be observed as a result, but our experimental resolution does not allow resolution of the  $2p_{1/2}$  and  $2p_{3/2}$  components, and this precludes any lineshape analysis in that case.

### 3.3. CVV Auger spectra

We mentioned earlier that the intrinsic widths of the Mn  $2p_{3/2}$ , Fe  $2p_{3/2}$ , and Co  $2p_{3/2}$  lines are smaller for the quasicrystalline phases (see the  $2\gamma$  values in table 1). This is equivalent to a longer lifetime of the  $2p_{3/2}$  core holes. As we first noted in [13], this correlates with a change in the Auger transition rates in the QCs as compared to the metals. The current extended database allows us to be more general here.

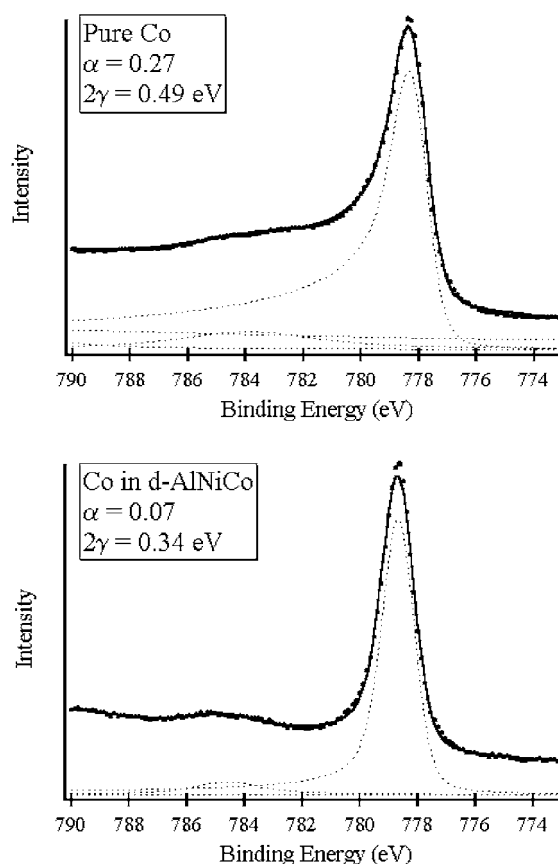
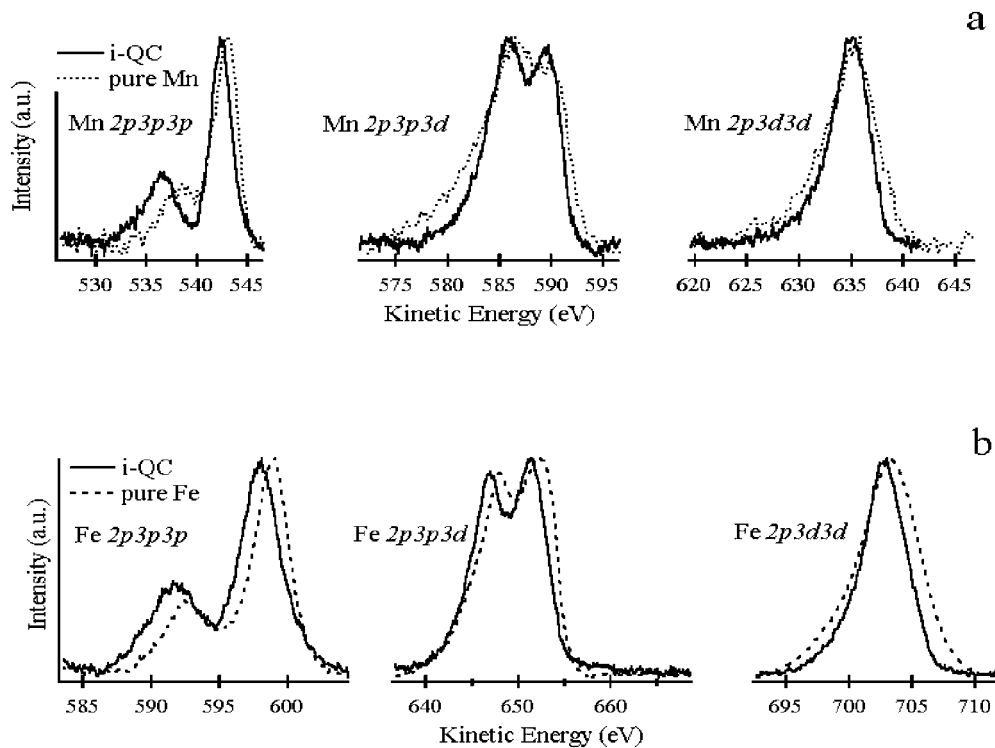


Figure 4. Co 2p<sub>3/2</sub> core levels in pure Co (top) and in d-Al<sub>72</sub>Ni<sub>11</sub>Co<sub>17</sub>.

For TMs, the lifetime is known to be determined essentially by the CVV Auger processes [35, 36]. Figure 5 compares the Mn and Fe CVV Auger lines for the pure metals and the i-QCs. The 2p and 3p levels can be considered as atomic in nature since they lie at high BEs. The 3d levels are valence states and therefore more sensitive to the chemical environment. It is therefore informative to compare the intensities of Auger lines that involve the 3d states with the intensities of Auger lines that involve only atomic states. We do this by evaluating the ratios  $A(2p3d3d/2p3p3p)$  and  $A(2p3p3d/2p3p3p)$ , where  $A$  is a ratio of areas of integrated peak intensities. We do this for both the pure metals and the i-QCs. For Mn, the ratios are about 3 and 7 respectively for the metal and reduced to about 2 and 5 for the QC. For Fe, the ratios are 1.9 and 2.3 respectively for the metal and reduced to 1.6 and 2.0 for the QC. This means that the rate of the electronic recombination processes of the 2p photohole involving a 3d electron is smaller in the QCs, by about 15–30%, depending on the alloy. This can be explained by an increased localization of the TM d states, which would reduce the probability of filling the photohole. The reduction of the intrinsic width of the Co 2p<sub>3/2</sub> line is expected to be related to a similar decrease of the 3d-containing Auger transition rates in the QC relative to the metal. Unfortunately, this is experimentally impossible to verify because of overlap between several Ni and Co Auger lines.



**Figure 5.** (a) Mn CVV Auger lines, in the  $N(E)$  mode, for the pure Mn (dashed curves) and for the  $i\text{-Al}_{72}\text{Pd}_{19.5}\text{Mn}_{8.5}$  QC (plain curves). (b) Fe CVV Auger lines, in the  $N(E)$  mode, for the pure Fe (dashed curves) and for the  $i\text{-Al}_{63.4}\text{Cu}_{24}\text{Fe}_{12.6}$  QC (plain curves). A Shirley background was subtracted.

The widths of the Mn and Fe  $2p3d3d$  lines are also smaller for the QCs than for the metals (4.0 eV versus 5.3 eV for Mn, 3.9 eV versus 5.4 eV for Fe), as can be seen in figure 5. The shape of this Auger line should reflect the self-convolution of the Mn and Fe 3d bands, and therefore the narrowing of the Auger line implies that the widths of the Mn and Fe 3d bands are smaller for the QC. This may shed some light on how the pseudogap opens in the QCs, as the distributions of the occupied Mn and Fe 3d states lie very close to  $E_F$  in  $i\text{-AlPdMn}$  and  $i\text{-AlCuFe}$ .

The Mn and Fe  $2p3p3d$  spectra should reflect the convolution of the 3d band with the 3p levels. The energy gap between the two components of the  $2p3p3d$  lines does not vary upon alloying. The two components are just better resolved as the result of the narrowing of the Mn or Fe 3d band in the QCs.

The final state of the  $2p3d3d$  Auger transition leaves two holes in the VB. In the 3d series of TMs, it has been observed that many-body final-state effects can lead to significant changes in the lineshape. This depends on the ratio between the energy cost of localizing two holes on the same atom (the correlation energy  $U$ ) and the VB width  $W$ . If  $U/W \ll 1$ , the Auger line remains an unshifted self-convolution of the VB corresponding to a delocalized, band-like final state. If  $U/W \gg 1$ , the Auger line appears shifted and atomic-like, with multiplet structure [37–40]. Figure 5 shows that, apart from a reduction in the bandwidth, the shape of the  $2p3d3d$  Auger line is essentially not different for the QCs to that for the metals, and its

position is only slightly shifted. Therefore, a band-like behaviour is still observed in the QCs, with no observable correlation effects.

In a recent publication, Hensch *et al* [41] presented some results on the CVV Auger lines of an  $i\text{-Al}_{70}\text{Pd}_{20}\text{Mn}_{10}$  QC surface prepared by different procedures leading to a surface termination having either a pentagonal, a decagonal, or a cubic symmetry. The position of the Mn 2p3d3d line appeared shifted by 0.75 eV for the pentagonal surface relative to the decagonal and cubic surfaces, while the BEs of the Mn 2p lines were unshifted. Using the measured BE of Mn 2p and the kinetic energy of the Mn 2p3d3d line, they derived the position of the Mn 3d band with respect to  $E_F$  in the QC. We recall that the kinetic energy of the Auger electron is given by

$$E_K(2p3d3d) = E_B(2p) - 2E_B(3d) - U. \quad (2)$$

Neglecting the variations of the correlation energy  $U$  between different structures, the authors concluded that the Mn 3d band is shifted by 0.9 eV toward higher BE in the pentagonal surface, suggesting a band filling in the QC.

While we believe that the idea of a partial band filling in the QC is correct, we do not believe that the positions of the Auger and XPS lines can be used to deduce this fact. This is because the correlation energy  $U$  in equation (2) cannot be neglected. By way of illustration, our data do not show any significant energy shift for either the Mn 2p or Mn 2p3d3d lines between the pure Mn and the  $i\text{-AlPdMn}$  surface. If we follow the same arguments as in [41] and simply neglect the values of  $U$ , then our data force us to conclude that the Mn 3d band lies at the same position with respect to  $E_F$  in the QC and in the metal, *in contradiction* with the idea of a band filling. In addition, we note that  $U$  is expected to vary significantly across the 3d series of TMs [37] and it seems therefore wrong to neglect its variation and, at the same time, infer a band filling from these observations, as this should produce variations of the correlation energy  $U$ . Finally, we mention that the idea that the Mn 3d band shifts from  $E_F$  in the QC has strong experimental support from SXES measurements [42]. There the energy distribution of the Mn 3d states is probed directly and its relative position with respect to  $E_F$  deduced from

$$E_B(3d) = E_B(2p) - [E_X(3d \rightarrow 2p)] \quad (3)$$

where  $E_X(3d \rightarrow 2p)$  is the energy of the x-ray transition resulting from the radiative recombination between a 3d electron and a 2p core hole. These SXES experiments show that the centre of the Mn 3d states lies about 1.1 eV below  $E_F$  and that the width of the band is narrower in the QC than in the metal. The experimentally derived position of the Mn 3d band also agrees with the electronic structure calculations performed on realistic approximants [43].

#### 4. Conclusions

Both Auger and core-level spectroscopies provide valuable information about specific features of the electronic structure of QCs. We were able to successfully fit the TM 2p core-level spectra of a set of ternary alloys in the  $\text{AlPdMn}$ ,  $\text{AlCuFe}$ , and  $\text{AlNiCo}$  ternary systems with the Doniach–Sunjic lineshape. The results show the systematic loss of the asymmetric tail in both the icosahedral and decagonal phases. For  $i\text{-AlPdMn}$ ,  $i\text{-AlCuFe}$ ,  $\xi'\text{-AlPdMn}$ , and  $o\text{-Al}_6\text{Mn}$ , a smaller  $\alpha$  can directly be correlated either with the VB spectra, where the pseudogap can be observed, or with a minimum in the calculated  $\text{DOS}(E_F)$ . On the other hand, the TM 2p core levels exhibit a large asymmetry in metallic systems like the pure metals or the cubic  $\text{AlPdMn}$  crystal, which is correlated with a large  $\text{DOS}(E_F)$ . Therefore our physical interpretation that the loss of the asymmetric tail arises from a reduced  $\text{LDOS}(E_F)$  seems to be rather solid. This effect was used to probe the  $\text{LDOS}(E_F)$  in various  $\text{AlPdMn}$  alloys and thereby observe how

the metallic character depends on the surface sensitivity and surface morphologies resulting from different methods of preparation [13].

We extended this core-level lineshape analysis to consider the still controversial issue of whether or not the AlNiCo decagonal phases are stabilized by a Hume-Rothery mechanism. The results indicate a reduced LDOS( $E_F$ ) around both Ni and Co atoms. In the case of Ni, the disappearance of the satellite structure provides evidence for a band-filling mechanism that shifts the Ni d band away from  $E_F$ . Altogether, our indirect approach to the pseudogap issue strongly supports an electronic stabilization in the AlNiCo decagonal phase.

Some more qualitative information was gained by the analysis of the CVV Auger spectra. On one hand, a smaller width of the Mn d and Fe d band in i-AlPdMn and i-AlCuFe QC relative to the pure metals can be inferred from the spectra. The shape of the 2p3d3d line still indicates a band-like behaviour, where the TM 3d valence electrons are delocalized (i). On the other hand, the reduction of the intrinsic width of 2p<sub>3/2</sub> levels (correlated with a decrease of the rate at which the 2p photoholes decay via the emission of the 3d electron) suggests an increased localization of the TM 3d valence electrons in the QCs relative to the pure metals (ii).

The qualitative conclusions (i) and (ii) seem to be contradictory. They can be placed in perspective using the recent work by Rotenberg *et al* [44] who observed some slightly dispersive bands in the vicinity of  $E_F$  for d-Al<sub>71.8</sub>Ni<sub>14.8</sub>Co<sub>13.4</sub> by angle-resolved PES. Their experiment rules out the existence of fully localized states characterized by an exponential decay of their amplitude as in amorphous systems. But this does not rule out the existence of critical states characterized by a power-law decay of their amplitude and predicted for a quasiperiodic potential. In that situation, the TM 3d electrons can still be delocalized but less easily than in a metallic system, and the apparent contradiction of conclusions (i) and (ii) can then be understood.

## References

- [1] Shechtman D, Blech I, Gratias D and Cahn J W 1984 *Phys. Rev. Lett.* **53** 1951
- [2] Dubois J-M, Brunet P and Belin-Ferré E 2000 *Quasicrystals: Current Topics* ed E Belin-Ferré, C Berger, M Quiquandon and A Sadoc (Singapore: World Scientific) pp 498–532
- [3] Mayou D, Trambly de Laissardière G and Cyrot-Lackmann F 1993 *Int. J. Mod. Phys. B* **7** 318
- [4] Mayou D, Cyrot-Lackmann F, Trambly de Laissardière G and Klein T 1993 *J. Non-Cryst. Solids* **153–4** 412
- [5] Fournée V, Belin-Ferré E and Dubois J-M 1998 *J. Phys.: Condens. Matter* **10** 4231
- [6] Rapp Ö 1999 *Physical Properties of Quasicrystals (Springer Series in Solid-State Sciences vol 126)* ed Z M Stadnik (Berlin: Springer) pp 127–67
- [7] Sire C and Gratias D 1994 Introduction to the physics of quasicrystals *Statics and Dynamics of Alloy Phase Transitions NATO ASI Series B vol 319*, p 127
- [8] Gardner M 1977 *Sci. Am.* **236** 110
- [9] Belin-Ferré E, Fournée V and Dubois J M 2000 *J. Phys.: Condens. Matter* **12** 8159
- [10] Hüfner S 1995 *Photoelectron Spectroscopy* (Berlin: Springer)
- [11] Boer J C 1981 *Solid State Commun.* **38** 1135
- [12] Weightman P 1995 *Microsc. Microanal. Microstruct.* **6** 263
- [13] Fournée V, Pinhero P J, Anderegg J W, Lograsso T A, Ross A R, Canfield P C, Fisher I R and Thiel P A 2000 *Phys. Rev. B* **62** 14 049
- [14] Delaney D W, Bloomer T E and Lograsso T A 1997 *New Horizons in Quasicrystals* ed A Goldman, D Sordelet, P Thiel and J M Dubois (Singapore: World Scientific) pp 45–52
- [15] Lograsso T A and Delaney D W 1996 *J. Mater. Res.* **11** 2125
- [16] Fisher I R, Kramer M J, Islam Z, Wiener T A, Kracher A, Ross A R, Lograsso T A, Goldman A I and Canfield P C 2000 *Mater. Sci. Eng. A* **A294–6** 10
- [17] Cai T, Fournée V, Lograsso T A, Ross A R and Thiel P A 2002 *Phys. Rev. B* at press
- [18] Ledieu J, McGrath R, Diehl R D, Lograsso T A, Delaney D W, Papadopolos Z and Kasner G 2001 *Surf. Sci.* **492** L729

- [19] Kishida M, Kamimura Y, Tamura R, Edagawa K, Takeuchi S, Sato T, Yokoyama Y, Guo J Q and Tsai A P 2002 *Phys. Rev. B* submitted
- [20] Fournée V, Belin-Ferré E, Pecheur P, Tobola J, Dankhazi Z, Sadoc A and Muller H 2002 *J. Phys.: Condens. Matter* **14** 87
- [21] Stadnik Z M 1999 *Physical Properties of Quasicrystals (Springer Series in Solid-State Sciences vol 126)* ed Z M Stadnik (Berlin: Springer) pp 127–67
- [22] Schaub T, Delahaye J, Berger C, Guyot H, Belkhon R, Taleb-Ibrahimi A and Calvayrac Y 2001 *Eur. Phys. J. B* **20** 183
- [23] Wertheim G K and Citrin P H 1978 *Photoemission in Solids* vol 26, ed M Cardona and L Ley (Berlin: Springer) pp 197–234
- [24] Sunjic S and Domiach A 1970 *J. Phys. C: Solid State Phys.* **3** 285
- [25] Kowalczyk S P, Ley L, McFeely F R and Shirley D A 1975 *Phys. Rev. B* **11** 1721
- [26] Shirley D A 1978 *Photoemission in Solids* vol 1, ed M Cardona and L Ley (Berlin: Springer) pp 165–96
- [27] Shen Z, Kramer M J, Jenks C J, Goldman A I, Lograsso T, Delaney D, Heinzig M, Raberg W and Thiel P A 1998 *Phys. Rev. B* **58** 9961
- [28] Stadnik Z M, Purdie D, Garnier M, Baer Y, Tsai A P, Inoue A, Edagawa K, Takeuchi S and Buschow K H J 1997 *Phys. Rev. B* **55** 10938
- [29] Trambly de Laissardière G, Mayou D and Nguyen Manh D 1993 *Europhys. Lett.* **21** 25
- [30] Neuhold G, Barman S R, Horn K, Theis W, Ebert P and Urban K 1998 *Phys. Rev. B* **58** 734
- [31] Hillebrecht F U, Fuggle J C, Bennet P A, Zolnierok Z and Freiburg C 1983 *Phys. Rev. B* **27** 2179
- [32] Stadnik Z M, Zhang G W, Tsai A P and Inoue A 1995 *Phys. Lett. A* **198** 237
- [33] Krajci M, Hafner J and Mihalkovic M 2000 *Mater. Sci. Eng. A* **294–6** 548
- [34] Fournée V, Belin-Ferré E, Sadoc A, Dankhazi Z, Muller H and Grushko B 2002 to be published
- [35] Vayrynen J 1981 *J. Electron Spectrosc. Relat. Phenom.* **22** 22
- [36] McGuire E J 1971 *Phys. Rev. A* **3** 1801
- [37] Cini M 1994 *J. Phys.: Condens. Matter* **6** 8549
- [38] Cini M 1976 *Solid State Commun.* **20** 605
- [39] Sawatzky G A 1977 *Phys. Rev. Lett.* **39** 504
- [40] Bennet P A, Fuggle J C and Hillebrecht F U 1983 *Phys. Rev. B* **27** 2194
- [41] Hensch A, Rossner B, Bolliger B and Erbudak M 2001 *Surf. Sci.* **489** 169
- [42] Belin E, Dankhazi Z, Sadoc A and Dubois J M 1994 *J. Phys.: Condens. Matter* **6** 8771
- [43] Häfner J 1999 *Curr. Opin. Solid State Mater. Sci.* **4** 289
- [44] Rotenberg E, Theis W, Horn K and Gilles P 2000 *Nature* **406** 602